FLOW ANALYSIS IN RIVER DANUBE BY FIELD MEASUREMENT AND 3D CFD TURBULENCE MODELLING

Sándor BARANYA and János JÓZSA

Department of Hydraulic and Water Resources Engineering,
Budapest University of Technology and Economics
H–1521 Budapest, Hungary
Phone: (+36-1) 463-1164, e-mail: baranya@vit.bme.hu

Received: April 3, 2006

Abstract

Spatial complexity of turbulent flow conditions has been investigated by means of ADCP measurements and CFD modelling in river Danube. The study area was a meandering river reach, characterized by shallows and strongly influenced by various river training works. High resolution bed survey and freezing plate sampling provided input river bed data for model implementation. The applied k-ε turbulence model could well reproduce velocity distributions measured in nature. Strong spatial variability of the velocity and turbulent kinetic energy fields demonstrated the necessity of 3D model approach under such fluvial conditions.

Keywords: ADCP, 3D CFD modelling, k-ε turbulence closure, Danube.

1. Introduction

In the Northwest Hungarian part of river Danube the lack of the dynamic equilibrium of the bed river training activities have been undertaken in the framework of which e.g. groin fields are widely used. Due to the complexity of the flow and morphodynamic conditions field investigations and related 3D CFD modelling started in 2002 aiming at maintaining favourable flow conditions wherever possible and improve unfavourable conditions at places in the light of the demands exposed by fluvial navigation. Extensive flow measurements were carried out by using Acoustic Doppler Current Profiler (ADCP), in addition to which a 3D CFD turbulence model was tested and implemented, utilizing the available high resolution digital terrain model based on recent river bed scanning.

The goal of the investigation is on one hand to see if currents with such a spatial complexity can be measured and then reasonably reproduced by proper numerical models, on the other hand to show that field measurement data and numerical flow models validated based on them offer a sound hydrodynamic basis for modelling sediment transport and bed morphology.

In this study a 4 km long reach of river Danube has been investigated with the above mentioned tools. In the paper first the 3D turbulence model will be presented including its theoretical and numerical bases, then the model results will be analysed including e.g. characteristic velocity fields, turbulent kinetic energy distributions and the comparison of measurable model results with ADCP field data.

2. Theory

In laboratory conditions free surface flows are in general investigated by means of hydraulic scale models based on the Froude-law, which takes inertia and gravity forces into account. This approach, however, can not properly take into account the effects of viscous forces resulting occasionally in significant difference between the Reynolds number of real and modelled flow conditions. Since flow features related to turbulence play a significant role in sediment transport processes, such models can not describe correctly these phenomena. On the contrary, proper numerical flow models supplied with high level turbulence closure modules do not need to be scaled, what means that these models can handle domains in their original extensions, as one of the clear advantages of such CFD models.

The numerical model used in this study is the CFD code called SSIIM (*Olsen*, 2002). SSIIM is an abbreviation for Sediment Simulation In Intakes with Multiblock option. It solves the Reynolds-averaged Navier-Stokes equations with the two-equation k-ε turbulence closure (see e.g. *Rodi*, 1984) in three space dimensions to compute the water flow using the finite volume approach as discretization method (see e.g. [8]).

The model uses the complete momentum equations in all the three directions thus resulting in a non-hydrostatic flow description. The governing equations are solved in a finite volume context by using the SIMPLE method [8] on a three-dimensional, non-orthogonal curvilinear structured grid.

The Reynolds-averaged Navier-Stokes equations are written in an Einstein-type summation form as follows:

$$\frac{\partial U_i}{\partial t} + U_j \frac{\partial U_i}{\partial x_j} = \frac{1}{\rho} \frac{\partial}{\partial x_j} \left(-P\delta_{ij} - \rho \overline{u_i u_j} \right),$$

where

- U: time-averaged velocity,
- u: velocity fluctuation,
- P: pressure,
- x_j: Cartesian space co-ordinates,
- δ_{ij}: Kronecker delta,
- ρ: fluid density.

The eddy viscosity concept with k-ε turbulence closure is used to model the Reynolds stress terms as follows:

$$-\rho \overline{u_i u_j} = \rho \nu_T \left(\frac{\partial U_i}{\partial x_j} + \frac{\partial U_j}{\partial x_i} \right) - \frac{2}{3} \rho k \delta_{ij},$$

where

ν_T: eddy viscosity coefficient,
k: turbulent kinetic energy.

The k turbulent kinetic energy is defined as

$$k \equiv \frac{1}{2}\overline{u_i u_i}.$$

Substituting the Reynolds stress terms into the Reynolds-averaged Navier-Stokes equations one obtains

$$\frac{\partial U_i}{\partial t} + U_j \frac{\partial U_i}{\partial x_j} = \frac{1}{\rho}\frac{\partial}{\partial x_j}\left[-\left(P + \frac{2}{3}k\right)\delta_{ij} + \nu_T \frac{\partial U_i}{\partial x_j} + \nu_T \frac{\partial U_j}{\partial x_i}\right].$$

In the model, in which ε represents the rate of turbulent energy dissipation, a transport equation is solved both for $k$and ε as a result of which the eddy viscosity coefficient can be evaluated as

$$\nu_T = c_\mu \frac{k^2}{\varepsilon}, \qquad (c_\mu = 0.09).$$

The transport of k is modelled by the following differential equation:

$$\frac{\partial k}{\partial t} + U_j \frac{\partial k}{\partial x_j} = \frac{\partial}{\partial x_j}\left(\frac{\nu_T}{\sigma_k}\frac{\partial k}{\partial x_j}\right) + P_k - \varepsilon,$$

where P_k defines the production of k, and this term is expressed as

$$P_k = \nu_T \frac{\partial U_j}{\partial x_j}\left(\frac{\partial U_j}{\partial x_i} + \frac{\partial U_i}{\partial x_j}\right).$$

The transport of ε is modelled by the following differential equation:

$$\frac{\partial \varepsilon}{\partial t} + U_j \frac{\partial \varepsilon}{\partial x_j} = \frac{\partial}{\partial x_j}\left(\frac{\nu_T}{\sigma_\varepsilon}\frac{\partial \varepsilon}{\partial x_j}\right) + C_{\varepsilon 1}\frac{\varepsilon}{k}P_k - C_{\varepsilon 2}\frac{\varepsilon^2}{k}.$$

The constant values of the k-ε turbulence model are [11]

C_μ =0.09
$C_{\varepsilon 1}$=1.44
$C_{\varepsilon 2}$=1.92
σ_k = 1.0
σ_ε = 1.3

The above equations are valid inside the fluid flow in the free turbulence zone, but next to the boundaries the flow characteristics are calculated from the following formula [12]:

$$\frac{U}{u_*} = \frac{1}{\kappa} \ln \left(\frac{30y}{k_s} \right),$$

where

U: velocity parallel to boundary layer,
u_* : friction velocity,
κ: von Karman constant,
y: distance between wall and the investigated point,
k_s: roughness height.

3. Case Study

3.1. Study River Reach

The investigated reach of river Danube is situated in Northwest Hungary between river kms 1792 and 1796 (*Fig. 1*). In this area the river is strongly influenced by various river training works such as groin fields, moreover, the river channel is meandering and characterized with a number of shallows.

The long term goal of the investigations is to support river training planning to provide sufficient depth even in low flow conditions for fluvial traffic, furthermore, to protect river banks from erosion. The channel bathymetry is very complex because of meandering resulting in scouring and bar formation, in which the river presents continuous change and evolution. One of the main causes of these phenomena is the hydropower plant at Bős (Gabcikovo) about 25 km upstream of the investigated reach, which once having been put into operation retains a significant part of sediment transport, especially the bead-load part of it. Another cause is a significant abrupt change in the longitudinal bottom slope of Danube located about 10 km upstream of the study reach. This means that the free surface slope decreases from 0.35 m/km to 0.15 m/km, so do consequently the kinetic energy and sediment transporting forces, resulting in considerable sediment deposits at places [9]. All that complexity required the launching of a detailed hydrodynamic investigation in the region.

At this part of the Danube the mean flow discharge is about 2000 m^3/s but in flood conditions it can grow even next to 10000 m^3/s as it happened in August 2002. Nevertheless, for fluvial navigation the critical period is low flow with discharge below 1400 m^3/s accompanied with drastic drop of the depth at places.

3.2. Field Measurements

The first step toward implementing the CFD model is to establish a reasonable digital terrain model. As an input for that the outcome of a recent ultrasonic bottom scanning was used. The scanning was carried out in spring 2002 at high flow

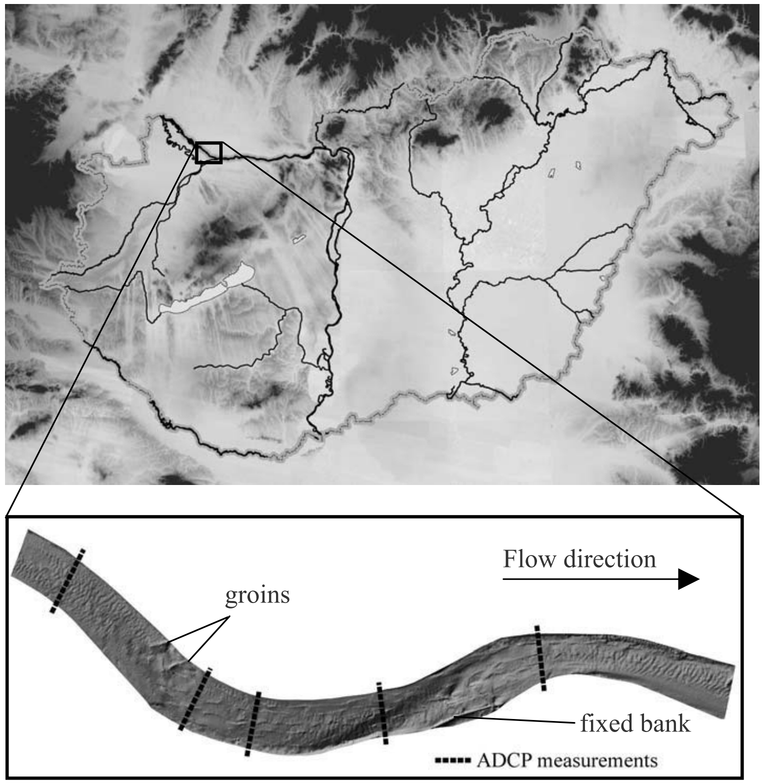

Fig. 1. Study river reach of Danube

conditions, providing high accuracy bathymetric data all over the main channel of the river. The scanner is mounted on a boat, which detects and records the bottom surface data by systematic cruising in the reach under investigation. The scattered data set on the bed surface are then used to generate the digital elevation model on a suitable grid.

In order to explore to some extent the distribution of the bed surface material and its texture in space and time, field sampling started in 2003 by applying a novel technology. It consists of using a freezing plate sampler, which uses low temperature liquid nitrogen gas for freezing a hemisphere of about 30 cm diameter of the bed surface layer right underneath the fixed sampler plate. An important outcome of this sampling is the determination of the grain size composition of the surface layer based on which the bed surface roughness can also be parameterized quite in a reasonable way.

In summer 2002 detailed flow measurements were carried out in the study river reach. Using the ADCP device, spatial distribution of the flow velocity and, as a by-product, cross-sectional bed profiles were taken in July at 1400 m^3/s, in August

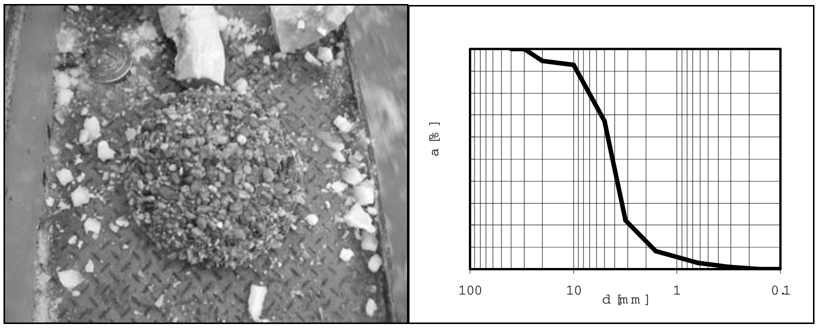

Fig. 2. a) Bed material sample *b*) Grain size distribution

at about 6000 m^3/s and in September at 1800 m^3/s discharge. These measurements were taken in the same 12 cross-sections in each case. Measuring one cross-section took approximately five minutes going across the river in a boat with the ADCP device mounted on board. For more details on the measuring methodology and data analysis, see e.g. [2].

Results from systematic ADCP measurements can make it possible to compare flow regime related changes in cross-section characteristics, varying a lot during even a single flood. Data can be used also as discharge type boundary conditions in numerical flow models. However, in this case the cross-sectional velocity distributions were utilized for validating the numerical flow model, as described later on in this paper.

3.3. Boundary Conditions

As it was mentioned in the previous chapter, one of the ADCP measurement campaigns was carried out at a discharge 1800 m^3/s, at about the shallows start to cause problems in fluvial navigation, making this flow regime particularly important to investigate. In the model the upstream boundary was thus set to 1800 m^3/s, whereas at the downstream boundary the water level was set to the value belonging to this discharge according to the local rating curve. Once setting the boundary conditions, the model was run until steady-state was reached.

Fig. 3 shows the applied grid, which has an average cell size of 30×15 meters. Taking the advantage of the boundary fitting capability of the grid, nodes were set also to the contour of groin (right figure) to describe the geometry correctly. In the vertical 10 layers the spacing was decreased toward the bottom where strong gradients were expected to occur in the flow variables.

A key model input is the parameterisation of the roughness. The model offers several options to define this hydraulic resistance feature, out of which the k_s [10] roughness height option was used. This can be calculated as $k_s = 3 \cdot d_{90}$, where

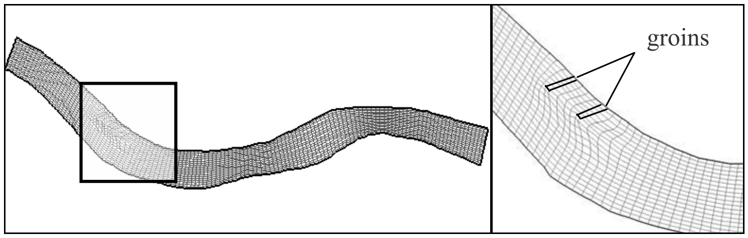

Fig. 3. Horizontal layout of the structured grid of the investigated river reach

d_{90} is the grain diameter above which 90% of the grains are retained.

For estimating k_s the results of the freezing plate bed sampling were used. From the grain size distribution (*Fig. 2b*) the approximate value k_s= 0.06 m was set in the model.

3.4. Model Results

Initial model testing was carried out by investigating flow conditions in a simple straight channel with a single groin [3]. The test runs showed the capability of the model to reproduce the essential of the expected spatial flow complexity in the near-groin region including e.g. recirculation zones both in the horizontal and the vertical plan.

3.4.1. Velocity Fields

Relevant results of numerical modelling are displayed here in the form of cross-sectional distributions, at the location identical to the ADCP measurements, facilitating direct comparisons and model validations. As to the model outcome, in a steady-state solution velocity fluctuations are not present at all in the time-averaged variables, as this effect is represented in a bulk way by the turbulent kinetic energy. On the contrary, ADCP measurements do contain such velocity irregularities due to the fast measuring technology. In order to imitate nature in that, fluctuation terms were added to the time-averaged velocity components in post-processing, calculating the extra terms based on the statistical relationship between turbulent kinetic energy and instantaneous fluctuation as follows (see e.g. [6]) :

$$u = \sqrt{\frac{2}{3}k} \cdot r,$$

where r: random number; a normal distribution with a mean of 0 and a standard deviation of 1.

The following *Figs. 4a-d* show velocity magnitudes in the selected cross-sections as were measured (right hand side) and numerically modelled (left hand side).

A fairly good agreement can be observed between measured and modelled velocity values. It is especially valid for the position of the highest flow velocities, which fall to the same zone in each section.

3.4.2. Turbulent Kinetic Energy

Turbulence conditions can be well characterized by turbulent kinetic energy distributions. *Fig. 5* shows k, in different cross-sections, as calculated by the numerical model. Locally significant turbulent kinetic energy representing in a way the sediment entrainment capacity close to the river bed can explain the usual development of scouring at the tip of the groins. The highest values generally develop in the line of highest velocities close to the bed surface. Note that the curved lining of the cross-sections at the groins is due to the necessary distortion of the grid lines to properly represent the groins, as seen in *Fig. 3*.

3.4.3. Secondary Currents

Removing the primary flow velocity vector component perpendicular to the cross-section the flow pattern is known as secondary flow developed in the cross-section plane can be made visible. As it is known, in a meandering channel this secondary flow shows a swirling behaviour. It can be explained e.g. by the irregular vertical distribution of the velocity. Since in general the velocity decreases moving toward the bottom, in a bent centrifugal forces acting on the upper layer become stronger than the ones acting on the lower layer, resulting in a net moment driving circulation in the span-wise plane. These flow patterns can be developed and easily seen in meandering rivers such as Danube. The following figures show velocity vectors in the span-wise plane in different locations.

3.4.4. Velocity Profiles

As it was mentioned before, in the numerical model the flow domain was discretized to 10 layers in the vertical. The model provided then velocity vectors in the centre of each layer. In addition, a surface velocity is also estimated that is why *Fig. 7* shows 11 points for model results for two selected locations. The circles represent results from ADCP field measurements. For one of the profiles the model results are perturbed by a scaled random component, as described earlier. Both profiles show reasonable logarithmic character. Due to the fast measuring capability of the ADCP, deviation might be of course high between time averaged and quasi-instantaneous

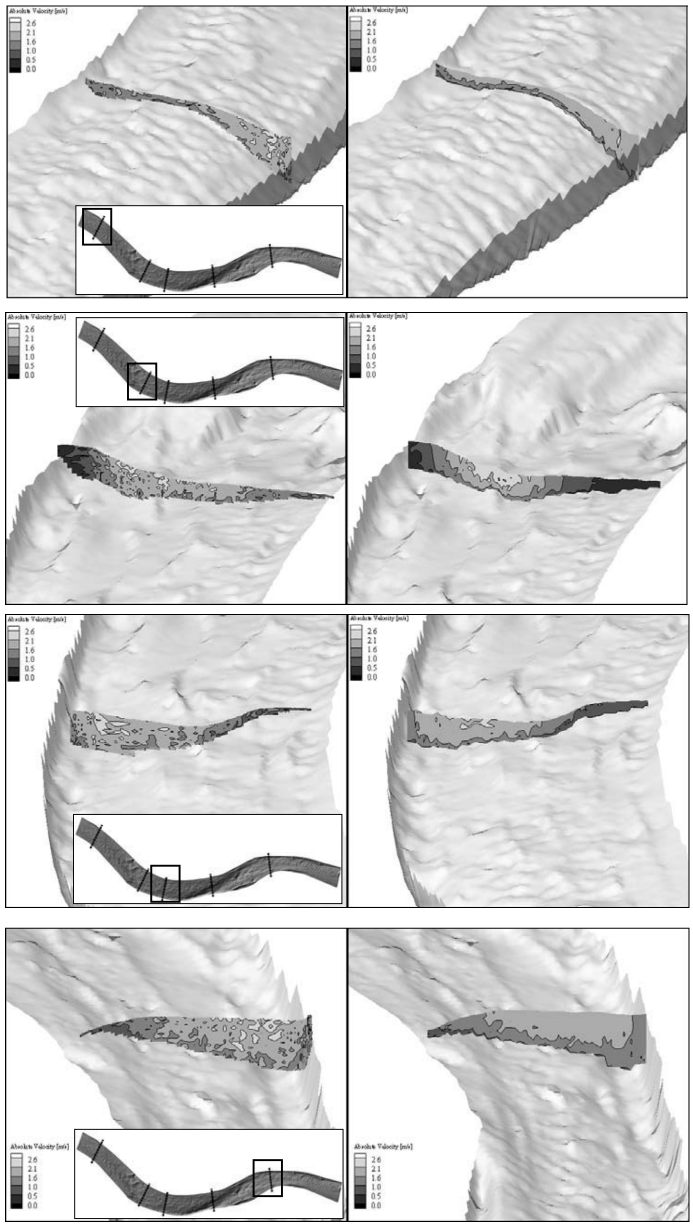

Fig. 4. $a) - d)$ Measured (left) and modelled (right) velocity magnitudes in selected cross-sections

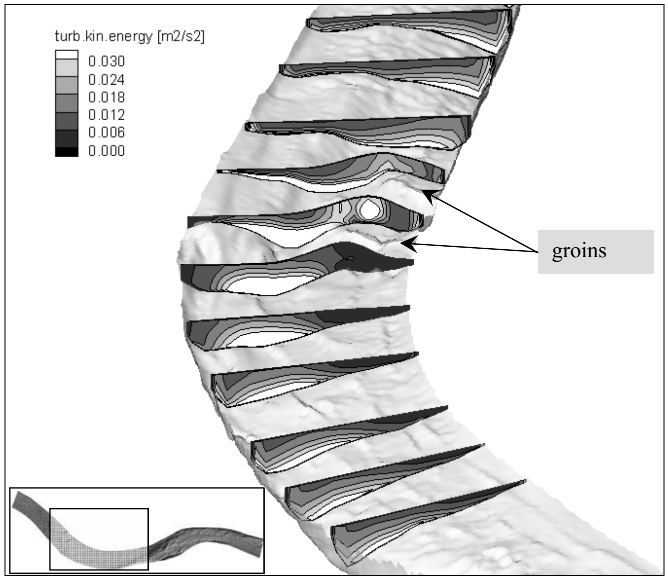

Fig. 5. Turbulent kinetic energy (k) fields

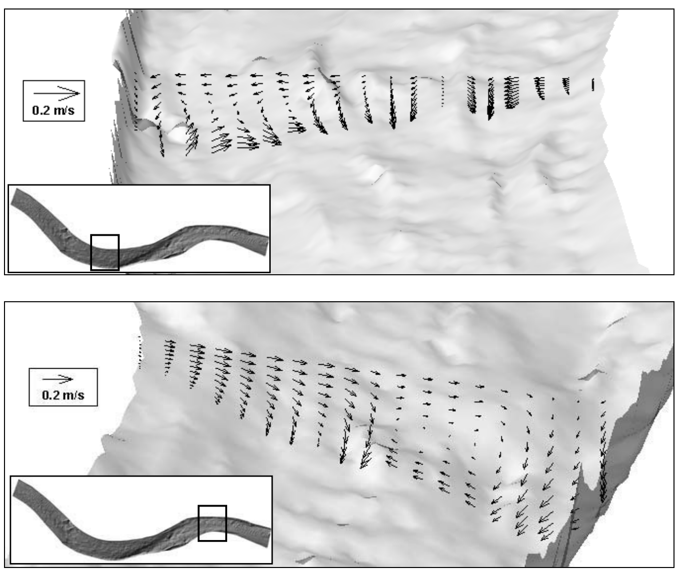

Fig. 6. Velocity vector components in the plane of perpendicular to the primary stream, showing secondary flow pattern

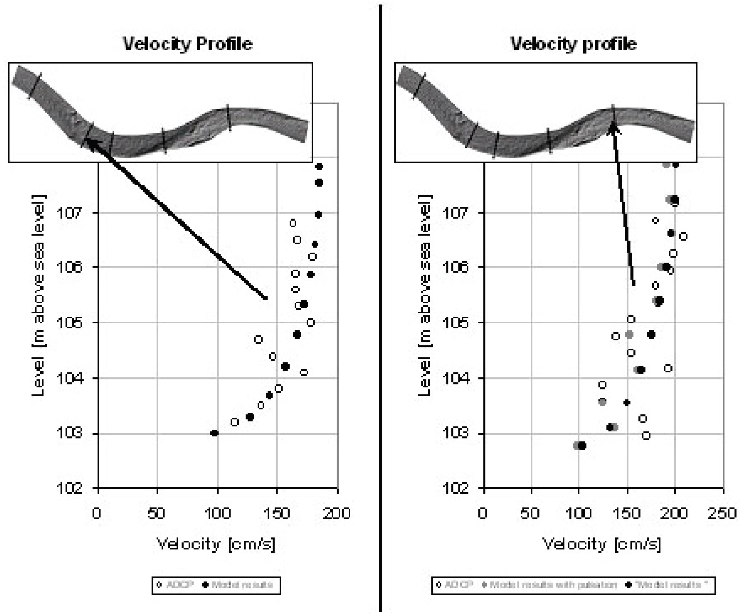

Fig. 7. a) – *b*) Vertical velocity profiles

values, but in this case good agreement can be seen between measured and modelled time averaged, steady-state values.

The lack of ADCP data close to the bottom and the free surface is due to the so-called blanking zone deficiency, for the time being unavoidable in the measurement technique.

4. Discussion

The chosen numerical turbulence model was successfully adopted to the study Danube reach. That velocity distributions measured in nature could be well reproduced in a river with complex bed geometry. Though in this stage of the research an overall roughness value was used, for improved tuning more detailed information is needed about bed surface texture and grain size composition, requiring systematic freezing plate sampling.

The strong spatial variability of velocity vectors and turbulent kinetic energy fields demonstrate the necessity of using three dimensional approach especially as the morphological changes in this reach are caused by bed-load sediment transport, thus making the accurate estimation of near bottom characteristics very important.

Acknowledgement

This work was part of the project 'Measurement and parameterization of free surface flows' No. T030792 supported by the National Scientific Research Fund of Hungary (OTKA).

References

[1] BARANYA, S., Flow Analysis at River Training Works by Means of 3D Turbulence Model: Application in River Danube between Győr and Gönyü (in Hungarian). MSc Dissertation, BME Department of Hydraulic and Water Resources Engineering, Budapest, 2003.

[2] BARANYA, S.– SOKORAY-VARGA, B., Investigation of the Spatial Features of Free Surface Flows by Means of ADP: First Application in River Danube (in Hungarian). Student research report, BME Faculty of Civil Engineering, Budapest, 2002.

[3] BARANYA, S. – JÓZSA, J., Investigation of Flow around a Groin with a 3D Numerical Model. CD-ROM *Proc. II. PhD CivilExpo*, Budapest University of Technology and Economics, Budapest, 2004.

[4] JÓZSA, J., Multidimensional Modelling of Flow and Transport in Surface Waters: Research – Application – Education in Hungary and abroad (in Hungarian). *Hidrológia Közlöny*, **81**, No. 4, Budapest, 2001.

[5] MARSON, C. – CARONI, E. – FIOROTTO, V. – DA DEPPO, L., Flow Field Analysis around a Groin. *Proc. XXX. IAHR Congress, Thessaloniki, Greece*, 2003.

[6] MONIN, A. S.– YAGLOM, A. M., Statistical Fluid Mechanics. MIT Press, Cambridge, Mass., USA, 1971.

[7] OLSEN, N. R. B., A Three-dimensional Numerical Model for Simulation of Sediment Movements in Water intakes with Moving Option. User's Manual, Department of Hydraulic and Environmental Engineering, The Norwegian University of Science and Technology, Trondheim, Norway, 2002.

[8] PATANKAR, S. V., Numerical Heat Transfer and Fluid Flow. McGraw-Hill Book Company, New York, 1980.

[9] RÁKÓCZI, L. – SASS, J., Changes of the Main Channel Bed of the Hungarian upper Danube and the Side Arms of Szigetköz Region due to Putting the Dunacsún I. barrage into operation (in Hungarian). *Vízügyi Közlemények*, LXXVII. évfolyam, 1-2. füzet, Budapest, 1995.

[10] RIJN, L. C. VAN, Sediment transport, Part I: Bed load transport. *Journal of Hydraulic Engineering, ASCE*, **110**, No. 10, 1984.

[11] RODI, W., Turbulence models and their application in hydraulics. State-of-the-art paper, IAHR Experimental and Mathematical Fluid Dynamics, 1984.

[12] SCHLICHTING, H., Boundary Layer Theory. McGraw-Hill, 1979.

[13] SONTEK Acoustic Doppler Profiler. Technical Documentation, San Diego, USA, 2001.

[14] YALIN, M. S., River Mechanics. Pergamon Press, Oxford, UK, 1992.